JOURNAL OF VIROLOGY, Oct. 2003, p. 11082–11093 Vol. 77, No. 20
0022-538X/03/$08.00+0 DOI: 10.1128/JVI.77.20.11082–11093.2003

Bioluminescence Imaging Reveals Systemic Dissemination of Herpes Simplex Virus Type 1 in the Absence of Interferon Receptors

Gary D. Luker,[1]* Julie L. Prior,[1] Jiling Song,[1] Christina M. Pica,[1] and David A. Leib[2]

Molecular Imaging Center, Mallinckrodt Institute of Radiology,[1] and Departments of Ophthalmology and Visual Sciences and Molecular Microbiology,[2] Washington University School of Medicine, St. Louis, Missouri 63110

Received 8 May 2003/Accepted 21 July 2003

Herpes simplex virus type 1 (HSV-1) can produce disseminated, systemic infection in neonates and patients with AIDS or other immunocompromising diseases, resulting in significant morbidity and mortality in spite of antiviral therapy. Components of host immunity that normally limit HSV-1 to localized epithelial and neuronal infection remain incompletely defined. We used in vivo bioluminescence imaging to determine effects of type I and II interferons (IFNs) on replication and tropism of HSV-1 infection in mice with genetic deficiency of type I, type II, or both type I and II IFN receptors. Following footpad or ocular infection of mice lacking type I IFN receptors, HSV-1 spread to parenchymal organs, including lung, liver, spleen, and regional lymph nodes, but mice survived. Deletion of type I and II IFN receptors produced quantitatively greatest and most widespread dissemination of virus to visceral organs and the nervous system, and these mice invariably died after ocular or footpad infection. Type II receptor knockout and wild-type mice had comparable viral replication and localization, with no systemic spread of HSV-1 or lethality. Therefore, while isolated deficiency of type II IFN receptors did not affect pathogenesis, loss of these receptors in combination with genetic deletion of type I receptors had a profound effect on susceptibility to HSV-1. These data demonstrate different effects of type I and II IFNs in limiting systemic dissemination of HSV-1 and further validate the use of bioluminescence imaging for studies of viral pathogenesis.

Herpes simplex virus type 1 (HSV-1) is a neurotropic human pathogen that typically initiates lytic infection at a local epithelial site, enters peripheral nerve terminals, and then is transported to sensory nerve ganglia. HSV-1 spread into the central nervous system can cause potentially fatal encephalitis, or virus may establish lifelong latent infection in ganglia. Although HSV-1 most commonly is limited to localized infection, virus also may disseminate widely to organs including lung, liver, and adrenals, particularly in neonates and patients with AIDS or other immunocompromising diseases (19, 30). Multiorgan infection with HSV-1 produces significant morbidity and mortality in spite of antiviral therapy (19). However, host immune responses that prevent systemic infection with HSV-1 remain incompletely defined.

Interferons (IFNs) are the major components of innate immunity to viral infection because they induce an antiviral state in infected cells and regulate the adaptive immune response to viruses (37). Type I IFNs, which predominantly include the 22 known isotypes of IFN-α and the single isotype of IFN-β, are secreted by most cells in response to viral infection (35), while production of type II IFN (IFN-γ) is restricted to activated T cells, natural killer (NK) cells, natural killer T cells, and dendritic cells (14, 15, 28). Each type of interferon binds to a distinct heterodimeric receptor, consisting of IFN-α receptor 1 (IFNAR1) and IFNAR2c for type I and IFN-γ receptor 1 (IFNGR1) and IFNGR2 for type II IFN. Receptors for type I and II IFNs are expressed on all nucleated cells (37). Binding of IFN to its cognate receptor initiates a signaling cascade that modifies the transcriptional and translational environment in cells, thereby conferring resistance to viral infection.

Previous studies in mice have documented the critical function of type I IFNs in host immunity to HSV-1. Depletion of type I IFNs with neutralizing antibodies produces marked increases in ocular virus titers following corneal infection (38), and replication of HSV-1 is significantly greater in the corneas and trigeminal ganglia of mice that lack type I IFN receptors (21). Similarly, treatment of mouse eyes with IFN-β reduces ocular titers of HSV-1 during acute infection and modestly inhibits establishment of viral latency in trigeminal ganglia (33). Conversely, the role of type II IFN in immunity to HSV-1 is more controversial. Depletion of type II IFN with neutralizing antibodies reduces clearance of virus (36), and HSV-1 infection has increased mortality in mice that lack type II IFN receptors (3). However, data from our laboratory and others have demonstrated that deficiency of type II IFN receptors has minimal effects on viral replication in eyes and trigeminal ganglia (2, 21). Synergistic inhibition of HSV-1 by type I and II IFNs also has been documented in mouse eyes treated with IFN-β and IFN-γ prior to viral infection (33). Importantly, these previous studies have not shown a role for IFNs in altering viral tropism or preventing systemic dissemination of virus.

We have recently shown that bioluminescence imaging of living mice can be used to monitor infection with an HSV-1 reporter virus (KOS/dlux/oriL) that expresses firefly luciferase (23). Differences in emitted light correlate with relative differences in virus titer, enabling noninvasive detection of viral replication and distribution over the course of infection. In the current study, we used bioluminescence imaging to investigate

* Corresponding author. Mailing address: Molecular Imaging Center, Mallinckrodt Institute of Radiology, Washington University School of Medicine, Box 8225, 4525 Scott Ave., Room 3324, St. Louis, MO 63110. Phone: (314) 362-9359. Fax (314) 362-0152. E-mail: lukerg@mir.wustl.edu.

changes in HSV-1 replication and tropism in mice genetically deficient in receptors for type I IFNs (IFN α/β $R^{-/-}$), type II (IFN γ $R^{-/-}$), or both type I and II interferons (IFN $\alpha/\beta/\gamma$ $R^{-/-}$). Following footpad or ocular infection of IFN $\alpha/\beta/\gamma$ $R^{-/-}$ mice, HSV-1 disseminated into numerous parenchymal organs, invariably resulting in lethality. Systemic spread of KOS/dlux/oriL was qualitatively less extensive and quantitatively lower in IFN α/β $R^{-/-}$ mice, while IFN γ $R^{-/-}$ and wild-type mice had only transient, limited extension of virus beyond the local site of infection. Importantly, IFN α/β $R^{-/-}$, IFN γ $R^{-/-}$ and wild-type mice all survived infection. These data demonstrated different effects of type I and II IFNs in limiting systemic dissemination of HSV-1 and showed that bioluminescence imaging can detect infection in unanticipated sites.

MATERIALS AND METHODS

Recombinant viruses. KOS/Dlux/oriL was constructed by homologous recombination into a site between UL49 and UL50 with a cassette encoding the UL30 promoter to regulate firefly luciferase as described previously (39). Virus stocks were propagated on Vero cells (32).

Mouse strains. All mice were in a pure 129 Ev/Sv background (referred to as wild type). Immunocompetent wild-type mice and mice deficient in type I IFN receptors (IFN α/β $R^{-/-}$), type II IFN receptors (IFN γ $R^{-/-}$), and both type I and II IFN receptors (IFN $\alpha/\beta/\gamma$ $R^{-/-}$) were provided by Skip Virgin (Washington University School of Medicine) (26). For selected experiments, wild-type mice and IFN γ $R^{-/-}$ mice were purchased from Taconic (Germantown, N.Y.) and the Jackson Laboratory (Bar Harbor, Maine), respectively.

Animal procedures. Animal handling procedures were approved by the Washington University School of Medicine Animal Studies Committee. Female mice 6 to 8 weeks old were anesthetized with ketamine and xylazine, and 50 μl of medium containing 2×10^5 or 2×10^6 PFU of KOS/Dlux/oriL was injected into footpads. Ocular infection with 2×10^6 PFU of KOS/Dlux/oriL in each eye was performed after corneal scarification as described previously (32). Before bioluminescence imaging on days 1 and 5 of experiments, the head, abdomen, and back of each animal were shaved to decrease attenuation and scattering of transmitted light by hair. For assays of acute infection, selected mice were euthanized for harvest of the following organs and tissues: liver, spleen, lung, kidney, brain, popliteal lymph nodes, blood, and a segment of spinal cord at the thoracolumbar junction. The serum fraction of blood was isolated with Samplette tubes (Sherwood Medical, St. Louis, Mo.). Organs were placed in 1 ml (spine, lymph nodes, blood, and serum), 3 ml (spleen, lung, kidney, and brain), or 5 ml (liver) of medium for homogenization with 1-mm beads (spine, lymph nodes) or 3-mm beads (all other organs) and sonication. Viral titers were determined on Vero cells and expressed as PFU per milliliter per gram of tissue weight.

Bioluminescence imaging. Imaging of firefly luciferase in mice was performed on a charge-coupled device camera (Xenogen Corp., Alameda, Calif.) as described previously (23). Briefly, 150 μg of D-luciferin (Xenogen Corp., Alameda, Calif.) was administered to mice by intraperitoneal injection. Mice were anesthetized with metofane or isoflurane, and imaging began 10 min after administration of D-luciferin. Anesthesia was maintained during imaging by nose cone delivery of anesthetic. Images were acquired for 1 to 120 s, depending on the amounts of light emitted from various sites of infection.

Quantification of bioluminescence imaging data. Relative intensities of transmitted light from in vivo bioluminescence were represented as a pseudocolor image ranging from violet (least intense) to red (most intense). Corresponding gray-scale photographs and color luciferase images were superimposed with LivingImage (Xenogen) and Igor (Wavemetrics, Lake Oswego, Oreg.) image analysis software. Data for photon flux from manually defined regions of interest were calculated as described previously (23). Area-under-the-curve (AUC) analyses of photon flux over the course of infection were performed with Kaleidagraph (Synergy Software, Reading, Pa.). Data are reported as mean values ± standard error of the mean for the number of animals indicated in the figure legends. Pairs were compared with Student's t test, and P values of ≤ 0.05 were considered significant.

RESULTS

Footpad infection with HSV-1 is lethal in IFN $\alpha/\beta/\gamma$ $R^{-/-}$ mice. To determine if signaling through IFN receptors affected tropism and spread of HSV-1, we injected footpads of wild-type, IFN α/β $R^{-/-}$, and IFN $\alpha/\beta/\gamma$ $R^{-/-}$ mice with 2×10^6 PFU of a recombinant strain KOS virus (KOS/dlux/oriL). The recombinant virus expresses firefly luciferase from the UL30 promoter, with a cassette inserted between UL49 and UL50 (39). Progression of acute infection over 10 days was monitored with bioluminescence imaging, using distribution and relative intensity of transmitted light to determine sites of infection and relative amounts of replicating reporter virus (23).

Luciferase activity was detected in the feet of all mouse genotypes on the first day postinfection, while no bioluminescence was identified in mock-infected mice (data not shown). In a limited number of animals from each group, dorsal images showed low levels of bioluminescence in the upper abdomen on day 1 postinfection. Abdominal bioluminescence likely was caused by injection of virus into small venous or lymphatic vessels during footpad infection, resulting in delivery of KOS/dlux/oriL to the liver (see below) (Fig. 1A). This idea was tested later in the current study with a mucosal (ocular) site of infection.

In a few wild-type mice, bioluminescence in the upper abdomen was seen transiently only on the first day postinfection. HSV-1 infection otherwise remained localized to the feet of wild-type mice on days 2 to 10 postinfection. Dorsal bioluminescence images showed small amounts of KOS/dlux/oriL in the upper abdomen of IFN α/β $R^{-/-}$ animals through approximately 6 days postinfection, although virus predominantly localized to feet of these mice. We could not detect luciferase activity in wild-type or IFN α/β $R^{-/-}$ mice by day 10, consistent with clearance of virus and establishment of latency. However, bioluminescence increased and spread rapidly in IFN $\alpha/\beta/\gamma$ $R^{-/-}$ mice, reaching the brain by 3 days postinfection. Unlike wild-type and IFN α/β $R^{-/-}$ animals, IFN $\alpha/\beta/\gamma$ $R^{-/-}$ mice all died within 4 days after footpad injection of KOS/dlux/oriL.

We have demonstrated previously that relative differences in virus titer at defined anatomic sites correlate with changes in bioluminescence measured by region-of-interest analysis (23). Region-of-interest data also enable small amounts of bioluminescence to be detected above background levels, even when light emission is below the threshold used for pseudocolor display. Therefore, we quantified KOS/dlux/oriL by region-of-interest analysis of light emitted from the feet, back, and heads of mice.

In all three regions, photon flux was greatest in IFN $\alpha/\beta/\gamma$ $R^{-/-}$ animals, demonstrating that the absence of both type I and II IFN signaling increased replication of HSV-1 (Fig. 1B to D). Bioluminescence in the feet of IFN $\alpha/\beta/\gamma$ $R^{-/-}$ mice was significantly greater than in the feet of IFN α/β $R^{-/-}$ animals on days 2 and 3 postinfection ($P < 0.05$) and wild-type mice on days 2 to 4 ($P < 0.01$). Differences between amounts of KOS/dlux/oriL in the feet of IFN α/β $R^{-/-}$ and wild-type animals were significant on days 2 to 6 ($P < 0.01$), before viral replication decreased rapidly in both genotypes. In the back and head regions of IFN $\alpha/\beta/\gamma$ $R^{-/-}$ mice, photon flux increased markedly in a time-dependent fashion, reaching levels that

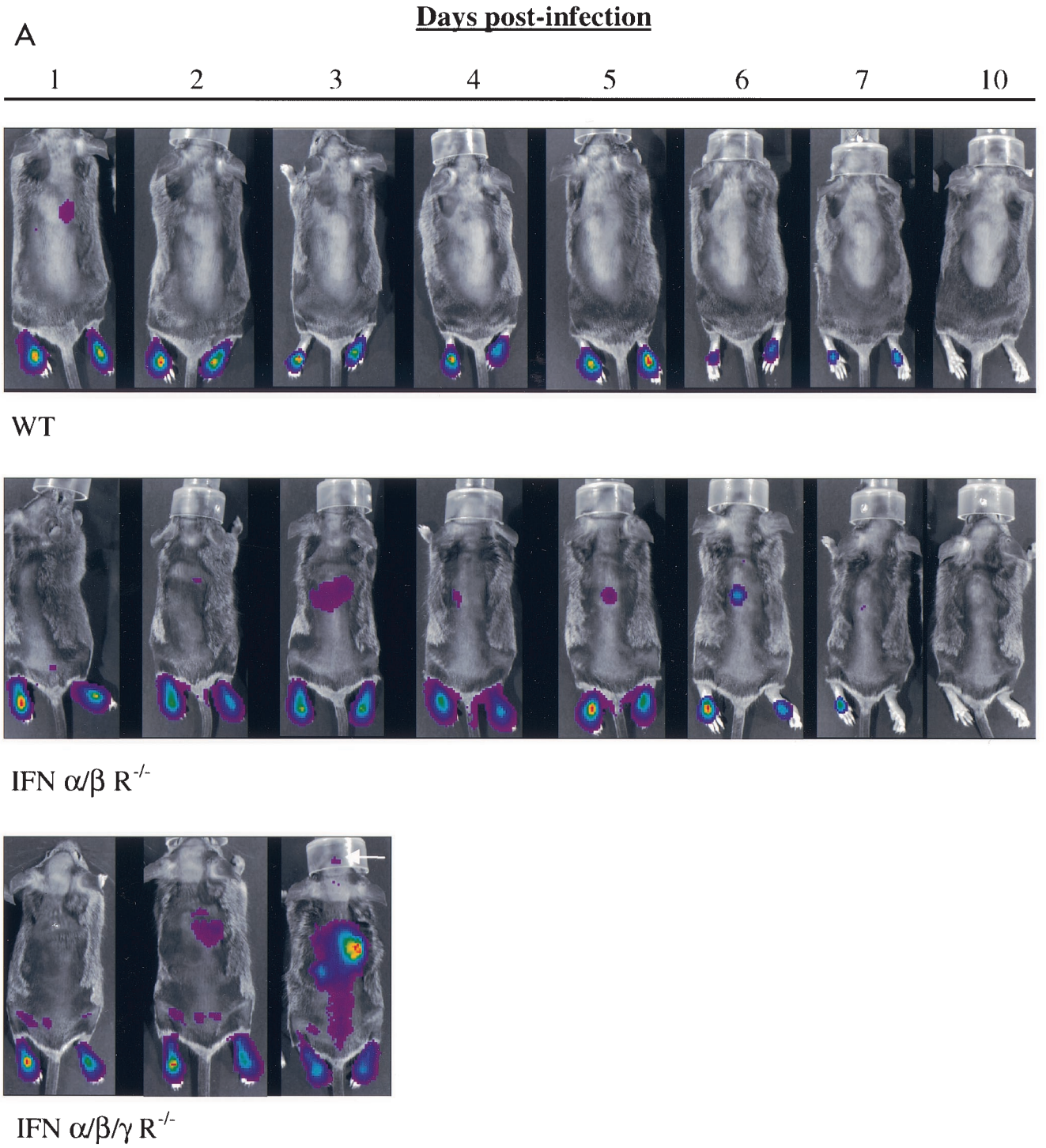

FIG. 1. Imaging replication and progression of HSV1 infection in wild-type (WT) SV129, IFN $\alpha/\beta/\gamma$ $R^{-}/^{-}$, and IFN α/β $R^{-}/^{-}$ mice (n = 5, 10, and 10, respectively) infected in the bilateral footpad with 2×10^6 KOS/dlux/oriL. Bioluminescence imaging was performed for 10 days postinfection with imaging times of 1 to 120 s, based on amounts of luciferase activity (A). Representative images from each mouse genotype are presented, with a uniform minimum threshold value for photon flux, but maximum values vary according to peak levels of bioluminescence for each genotype of animal. The white arrow shows light emission from the head of the IFN $\alpha/\beta/\gamma$ $R^{-}/^{-}$ mouse on day 3 postinfection. Photon flux was quantified from region-of-interest analysis of the feet (B), back (C), and head (D). Photon flux values of 10^2 in this experiment are background levels for the imaging system. Data are plotted as mean values ± standard error of the mean in these and subsequent figures. For many data points, error bars are smaller than the symbol. The AUC for bioluminescence from the feet (E), back (F), and head (G) was calculated over 4 days postinfection, corresponding to the survival time of IFN $\alpha/\beta/\gamma$ $R^{-}/^{-}$ mice.

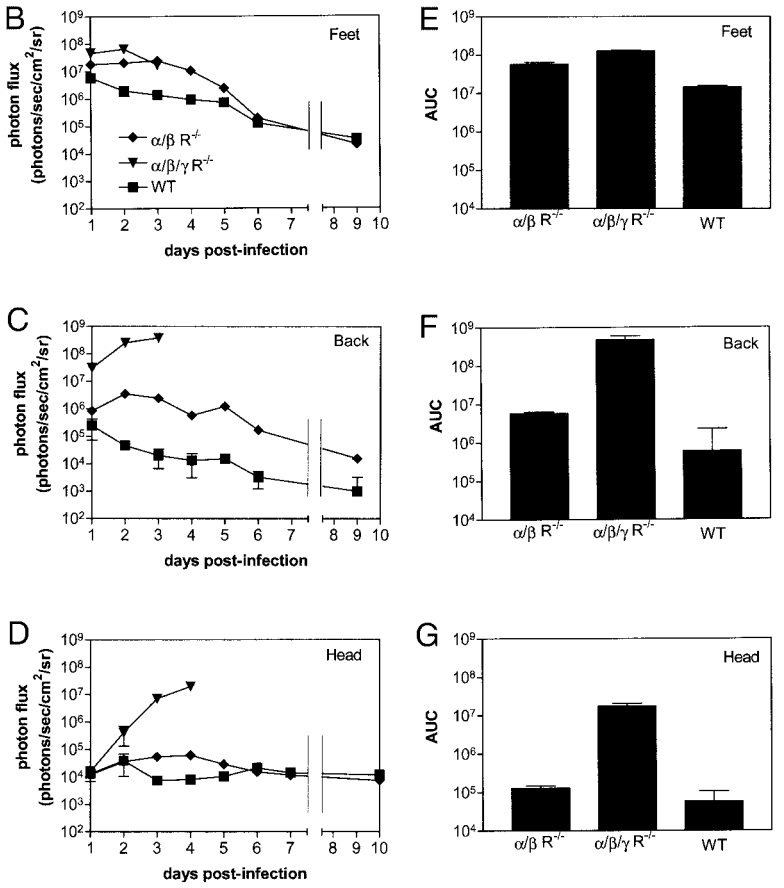

FIG. 1—*Continued.*

were 2 to 4 logs greater than in the other genotypes of mice ($P < 0.001$). Compared with wild-type mice, bioluminescence measured from the backs and heads of IFN α/β $R^{-/-}$ mice was higher on days 3 to 10 ($P < 0.005$) and 3 to 5 ($P < 0.01$) postinfection, respectively. In wild-type animals, photon flux from the head regions of interest was essentially at background levels throughout the course of infection.

To further analyze the effects of IFN on HSV-1 infection, we analyzed photon flux data by area-under-the-curve (AUC) analysis at each site (Fig. 1E to G). Over the 4-day period that IFN $\alpha/\beta/\gamma$ $R^{-/-}$ mice survived, the AUC for these animals was significantly higher than for IFN α/β $R^{-/-}$ and wild-type in the feet ($P < 0.01$), back ($P < 0.005$), and head ($P < 0.001$). Absence of type I IFN receptors increased the amounts of virus in all regions relative to wild-type mice during the first 4 days postinfection ($P < 0.01$) and the full 10-day course of imaging (data not shown). Overall, these results showed that type I IFNs limit replication and spread of HSV-1, but both type I and II IFNs were essential to prevent lethal infection.

Deficiency of type II IFN receptors has no effect on viral replication or spread from footpads. In the absence of type I IFN receptors, our data demonstrated an essential function for type II IFN in clearance of disseminated HSV-1 infection. Therefore, we determined if isolated deficiency of type II IFN receptors affected the progression or spread of infection. We infected the footpads of wild-type and IFN γ $R^{-/-}$ mice with KOS/dlux/oriL and monitored viral replication by bioluminescence imaging. As determined by region-of-interest analysis and AUC calculations, viral replication in footpads over 10 days was slightly higher in wild-type than in IFN γ $R^{-/-}$ mice (Fig. 2A and data not shown). Transient spread of virus beyond the feet was detected in a few mice of each genotype on day 1 postinfection, although the AUC of photon flux quantified from the backs of these mice did not differ significantly (Fig. 2B). None of these animals had persistent dissemination of HSV-1 or died from infection. Overall, these data established that isolated deficiency of type II IFN receptors did not permit systemic spread of HSV-1 following footpad infection.

Localization of luciferase activity in wild-type and IFN receptor-deficient mice. HSV-1 typically produces localized epithelial infection with retrograde transport of virus to innervating sensory neurons. The distribution of bioluminescence in IFN $\alpha/\beta/\gamma$ $R^{-/-}$ mice following footpad infection did not conform solely to a pattern consistent with neurotropic spread of virus to the spinal cord and brain. Because bioluminescence images are two-dimensional, light detected from the upper abdomen on dorsal images potentially could arise from more than one superimposed or adjacent organ or tissue, with relatively greater light emission from sites closer to the charge-coupled device camera. This limitation on spatial localization of luciferase activity may be overcome by imaging animals from more than one projection.

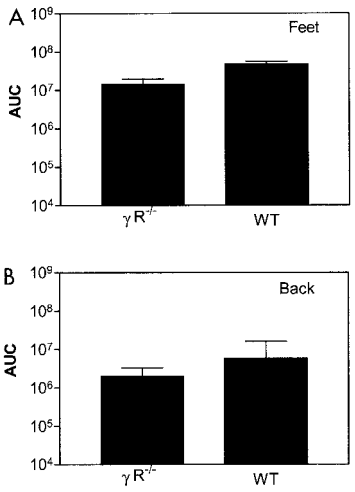

FIG. 2. AUC analysis of photon flux in the feet (A) and back (B) of wild-type (WT) ($n = 5$) and IFN γ $R^{-/-}$ ($n = 10$) mice imaged for 10 days after bilateral footpad injection of 2×10^6 KOS/dlux/oriL.

To more precisely localize KOS/dlux/oriL in IFN α/β/γ $R^{-/-}$ mice, we imaged animals in dorsal, ventral, and left lateral positions 2 and 3 days after footpad infection (Fig. 3A to C and data not shown). By analyzing different imaging projections, exploiting the fact that light emission is attenuated approximately 10-fold per cm of tissue (7), and comparing sites of luciferase activity with known mouse anatomy, we detected virus in expected positions of the liver, spleen, kidneys, spine, brain, and draining popliteal lymph nodes. Therefore, imaging data showed that IFN α/β/γ $R^{-/-}$ mice had widespread viral infection in multiple organs and suggested that the luciferase activity seen in the upper abdomen of the other genotypes of mice could arise from sites besides the spine, such as the liver.

To better identify sites of infection in IFN α/β/γ $R^{-/-}$ mice, we performed a limited dissection of a luciferin-injected animal immediately after sacrifice and used bioluminescence imaging to detect luciferase activity in excised organs and tissues (Fig. 3D and Fig. 3E). Bioluminescence was present in the spine, brain, spleen, and liver, confirming data obtained in intact animals. Luciferase activity was also detected in lungs and multiple sites in the thorax and abdomen, possibly arising from infected lymph nodes. Infection in these tissues was not prospectively identified on images from intact animals, likely because high levels of bioluminescence in adjacent liver and spleen overlapped light emission from lung and lymph nodes. We detected only very low levels of light emission from isolated kidneys (data not shown), probably due to delays in imaging this organ relative to decay of the bioluminescence signal.

To correlate imaging data with virus titers in mice with disseminated infection, we harvested selected organs and tissues 2 days after footpad infection in IFN α/β/γ $R^{-/-}$ mice, corresponding to the first day that KOS/dlux/oriL could be detected outside of the feet by imaging. We also quantified virus titers by plaque assay 3 days postinfection in wild-type, IFN α/β/γ $R^{-/-}$, IFN α/β $R^{-/-}$, and IFN γ $R^{-/-}$ animals. On day 2, the highest titers of HSV1 in IFN α/β/γ $R^{-/-}$ mice were detected in the spleen, while smaller amounts of virus were present in the liver and spine (Fig. 4). Significant titers were also observed in the popliteal lymph nodes, blood, and serum of these mice on day 2 postinfection (data not shown). Three days postinfection, virus titers in IFN α/β/γ $R^{-/-}$ mice increased in the spleen, liver, and spine. Virus was also detected in the lungs, kidneys, and brain.

Analysis of IFN α/β $R^{-/-}$ mice confirmed that these animals also had disseminated HSV-1 infection, although virus titers were significantly lower ($P < 0.001$) and detectable only in the liver, spleen, and kidney. Virus could not be detected in any of these organs in wild-type or IFN γ $R^{-/-}$ animals. Overall, the results for virus titers confirmed the qualitative and quantitative bioluminescence imaging data that showed widespread infection in IFN α/β/γ $R^{-/-}$ mice, less extensive dissemination in IFN α/β $R^{-/-}$ animals, and only localized infection in wild-type and IFN γ $R^{-/-}$ mice.

Reduced input titer of KOS/dlux/oriL also produces disseminated lethal infection in IFN α/β/γ $R^{-/-}$ mice. To determine if IFN α/β/γ $R^{-/-}$ mice would be susceptible to a reduced viral inoculum, we injected the footpads of these animals with 2×10^5 or 2×10^6 PFU of KOS/dlux/oriL. We initially imaged mice at 7.5 h postinfection and then performed bioluminescence imaging twice daily for days 1 to 3 postinfection to improve temporal monitoring of viral replication and spread. Imaging data for the feet, back, and head showed higher photon flux at each time point for mice injected with the higher titer, although differences in bioluminescence in the feet were modest (Fig. 5A to C). Spread of infection beyond the feet was delayed in mice that received 2×10^5 PFU, but amounts of virus continued to increase in both groups of IFN α/β/γ $R^{-/-}$ mice. Infection was invariably lethal on day 3 or 4 postinfection for animals injected with 2×10^6 or 2×10^5 PFU, respectively. Independent of the starting amount of virus, all mice developed disseminated infection to the same anatomic sites in parenchymal organs, lymph nodes, and the nervous system. These data demonstrated that a 10-fold reduction in viral inoculum still produced disseminated, lethal infection in mice lacking type I and II IFN receptors.

Corneal infection of IFN receptor-deficient mice. We considered that footpad injection potentially could introduce virus directly into small lymphatic or blood vessels, thereby promoting systemic spread of HSV-1. To determine if HSV-1 disseminated from a mucosal surface, we used the corneal model of infection and assayed the infection by bioluminescence imaging for 8 days (Fig. 6A). In wild-type mice, virus was initially detected only in the eyes, followed by spread to expected positions of trigeminal ganglia and overlying periocular tissues. Imaging data reproduced the known progression of acute HSV-1 infection from the cornea to the trigeminal ganglia, with subsequent zosteriform return to periocular skin (23, 40). Bioluminescence from KOS/dlux/oriL was essentially undetectable by day 8 postinfection, which is consistent with the expected time course for latency in wild-type animals. Similar to our results for footpad injections, ocular infection of IFN γ $R^{-/-}$ mice with KOS/dlux/oriL produced a time course and localization of virus that was comparable to these in wild-type animals. Importantly, neither wild-type nor IFN γ $R^{-/-}$mice showed systemic dissemination of virus or died from acute infection.

IFN α/β $R^{-/-}$ animals also had the expected progression of

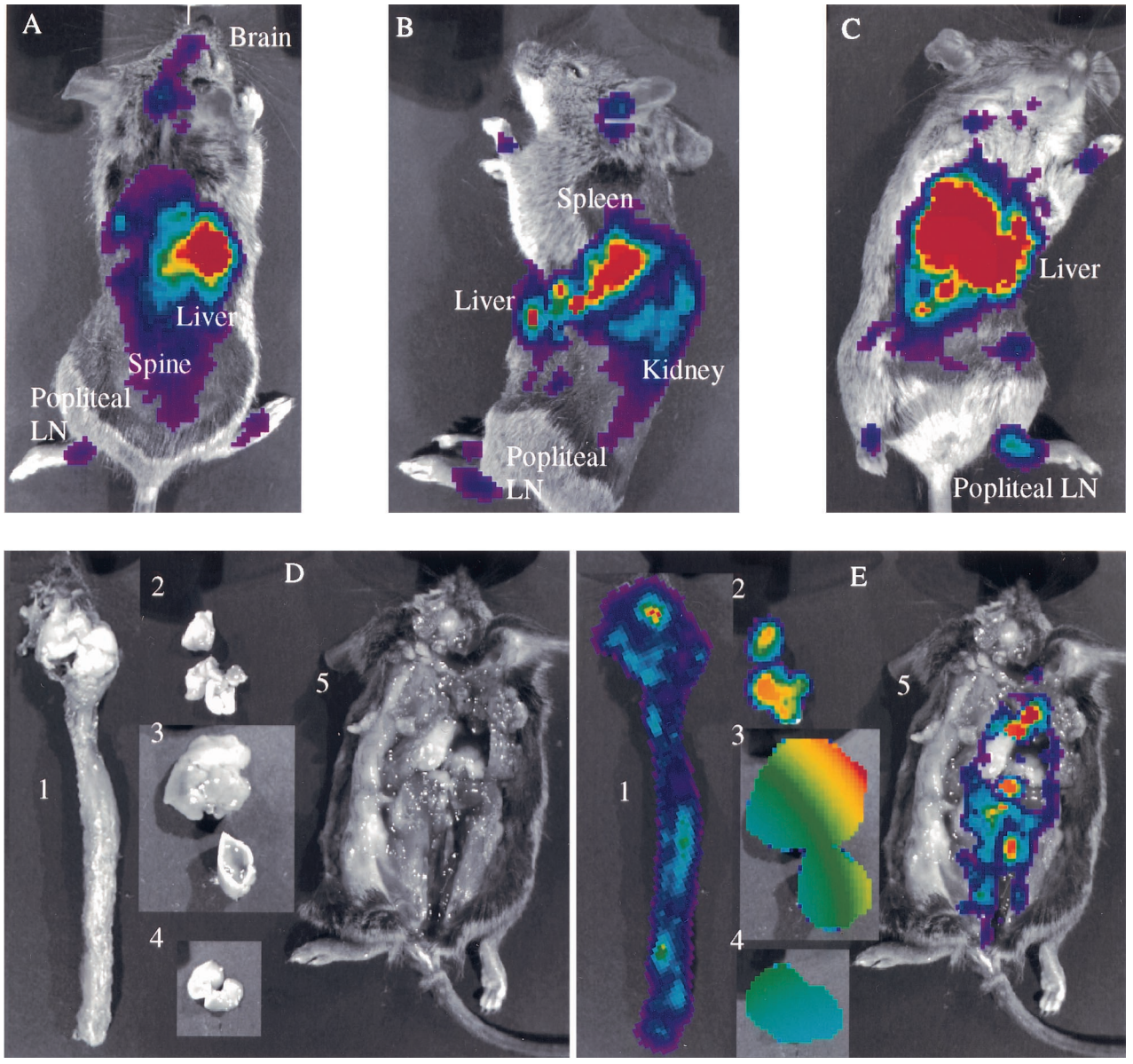

FIG. 3. Localization of bioluminescence activity in parenchymal organs of a representative IFN $\alpha/\beta/\gamma$ $R^{-/-}$ mouse 3 days after bilateral footpad infection with 2×10^6 KOS/dlux/oriL. Bioluminescence imaging was performed for 1 min each in dorsal (A), left lateral (B), and ventral (C) projections. Immediately after imaging, limited dissection was performed to isolate organs for ex vivo bioluminescence imaging. Gray-scale (D) and 1-min bioluminescent (E) images were obtained for the spine and brain, lungs, liver, spleen, and body cavity (images 1 to 5, respectively). Labeled organs and tissues in panels A to C were verified by ex vivo luciferase activity and/or plaque assay for virus. LN, lymph node.

acute infection in the eyes and periocular tissues. However, KOS/dlux/oriL was detected in the ventral aspect of the neck on day 2 postinfection in both IFN α/β $R^{-/-}$ and IFN $\alpha/\beta/\gamma$ $R^{-/-}$ mice, and virus was clearly evident within abdominal organs by day 3. While comparable sites were infected in both genotypes of mice, overall distribution of virus within the abdomen was more extensive in IFN $\alpha/\beta/\gamma$ $R^{-/-}$ than IFN α/β $R^{-/-}$ mice. In IFN α/β $R^{-/-}$ animals, bioluminescence was cleared from the abdomen by day 5 postinfection, which was earlier than observed in the head and neck. All IFN α/β $R^{-/-}$ mice survived ocular infection with KOS/dlux/oriL. By comparison, none of the IFN $\alpha/\beta/\gamma$ $R^{-/-}$ mice lived more than 4 days postinfection.

To quantify relative amounts of virus at the site of infection, we measured total photon flux in the head by region-of-interest analysis (Fig. 6B). On the initial 4 days postinfection, rank order of head bioluminescence was IFN $\alpha/\beta/\gamma$ $R^{-/-}$ > IFN α/β $R^{-/-}$ > IFN γ $R^{-/-}$ $\cong$ wild-type mice. Photon flux from IFN $\alpha/\beta/\gamma$ $R^{-/-}$ and IFN α/β $R^{-/-}$ animals was significantly greater than that from IFN γ $R^{-/-}$ and wild-type mice on each day analyzed ($P < 0.001$). Peak bioluminescence occurred on days 5 to 6 for wild-type, IFN α/β $R^{-/-}$, and IFN γ $R^{-/-}$ mice,

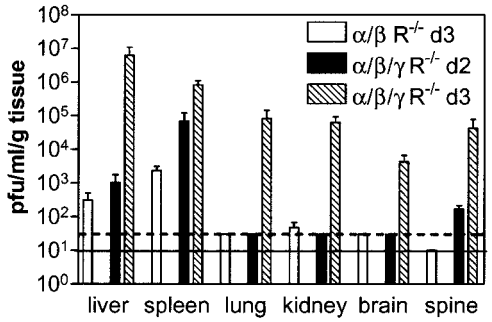

FIG. 4. Plaque assays of virus titers in selected organs and tissues of IFN $\alpha/\beta/\gamma$ $R^{-/-}$ and IFN α/β $R^{-/-}$ mice harvested 2 or 3 days after footpad infection with 2×10^6 KOS/dlux/oriL. Data are presented as mean values ± standard error of the mean. The dashed line shows the limit of detection (30 PFU/ml/g of tissue) for spleen, lung, kidney, and brain. The solid line denotes the limit of detection (10 PFU/ml/g of tissue) for the spine. The sensitivity for detection of virus in the liver was 500 PFU/ml/g of tissue. There were four IFN $\alpha/\beta/\gamma$ $R^{-/-}$ mice on day 3, and two mice each for IFN $\alpha/\beta/\gamma$ $R^{-/-}$ on day 2 and for IFN α/β $R^{-/-}$ on day 3 postinfection.

consistent with the expected time course of zosteriform spread of virus to periocular tissues. Photon flux subsequently declined in the three genotypes of mice that survived acute infection. By AUC analysis, IFN $\alpha/\beta/\gamma$ $R^{-/-}$ and IFN α/β $R^{-/-}$ mice had comparable amounts of head bioluminescence, and values for both genotypes were significantly greater than for IFN γ $R^{-/-}$ and wild-type mice ($P < 0.001$) (Fig. 6C). By comparison, the AUC for IFN γ $R^{-/-}$ mice did not differ from that for wild-type mice.

Region-of-interest analysis confirmed that abdominal bioluminescence was not detectable above background levels until day 3 postinfection in IFN $\alpha/\beta/\gamma$ $R^{-/-}$ or IFN α/β $R^{-/-}$ mice (Fig. 6D). Photon flux peaked at day 4 in IFN $\alpha/\beta/\gamma$ $R^{-/-}$ animals, after which time these mice died from HSV-1 infection. Peak levels of abdominal bioluminescence in IFN $\alpha/\beta/\gamma$ $R^{-/-}$ animals were nearly 2 logs greater than the highest amounts observed in the heads of infected mice, demonstrating extensive dissemination of virus beyond the local site of ocular infection. Abdominal photon flux in IFN $\alpha/\beta/\gamma$ $R^{-/-}$ mice was significantly greater than in IFN α/β $R^{-/-}$ on days 3 and 4 postinfection ($P < 0.01$ and 0.001, respectively). In IFN α/β $R^{-/-}$ mice, bioluminescence from abdominal sites remained constant on days 3 and 4 and then decreased to background levels by day 6. No detectable light emission above background could be detected outside the heads of IFN γ $R^{-/-}$ or wild-type mice at any time during infection. By AUC analysis, abdominal photon flux in IFN $\alpha/\beta/\gamma$ $R^{-/-}$ mice was significantly greater than in all other genotypes ($P < 0.001$), and bioluminescence in IFN α/β $R^{-/-}$ animals was higher than in IFN γ $R^{-/-}$ or wild-type mice ($P < 0.001$) (Fig. 6E).

To better define anatomic sites infected with KOS/dlux/oriL, we imaged mice from dorsal, ventral, and both lateral positions. Based on sites in which virus was detected following footpad infection and correlation with mouse anatomy, we determined probable organs and tissues in IFN $\alpha/\beta/\gamma$ $R^{-/-}$ mice that were infected with virus 4 days after ocular inoculation (Fig. 6F). Within the abdomen, bioluminescence was detected in expected positions of the liver, spleen, and kidneys, while light in the head and neck corresponded with eyes, periocular tissues, and submandibular and cervical lymph nodes. Temporal progression of infection as determined by imaging suggested the following route for systemic dissemination of KOS/dlux/oriL: eyes → submandibular and cervical lymph nodes → systemic circulation in blood and lymphatic vessels → parenchymal organs. Overall, these qualitative and quantitative bioluminescence data confirmed the results with footpad infection, showing that type I IFN receptors were necessary to prevent systemic dissemination of HSV-1. In the context of type I IFN receptor deficiency, type II receptors limited viral replication and prevented lethality, although isolated deletion of type II IFN receptors had no significant phenotype in acute HSV-1 infection.

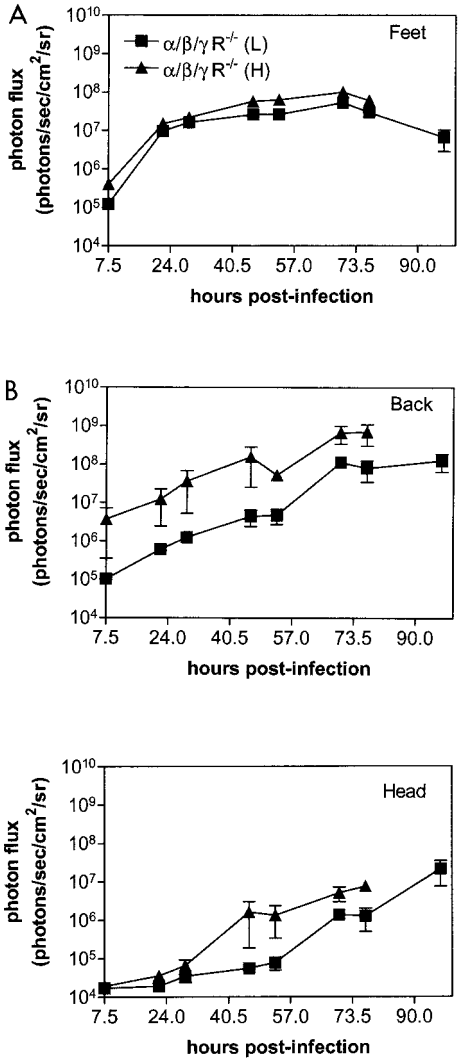

FIG. 5. Photon flux determined by region-of-interest analysis of the foot (A), back (B), and head (C) regions of IFN $\alpha/\beta/\gamma$ $R^{-/-}$ mice infected in the bilateral footpads with 2×10^5 (low, L) or 2×10^6 (high, H) KOS/dlux/oriL. Bioluminescence imaging was performed over the full course of infection in each group of mice, with lethality occurring on day 3 (high) or 4 (low) postinfection.

DISCUSSION

HSV-1 and other alphaherpesviruses typically produce localized infections in which virus replicates primarily in epithelial cells, spreads into innervating sensory neurons, and establishes latency in sensory nerve ganglia. While the importance of host interferons and viral regulators of the interferon response to infection have been well characterized (18, 20), defects in adaptive cellular immunity have been associated more closely with severe herpes simplex virus infection and disseminated disease in humans (16, 42, 43). Hence, the roles of interferons and other components of the innate immune response in preventing systemic infection with HSV-1 have not been defined.

The current study showed that the absence of type I IFN receptors permitted dissemination of HSV-1 to parenchymal organs and lymph nodes, in addition to the expected progression of infection from epithelia to neurons, following localized ocular or footpad infection. Although systemic infection with HSV-1 is frequently associated with mortality (19), IFN α/β $R^{-/-}$ animals ultimately cleared acute infection and survived. Deficiency of both type I and II IFN receptors produced qualitatively more extensive and quantitatively greater dissemination of virus, and infection was always fatal in these mice. By comparison, isolated deficiency of type II IFN receptors did not significantly affect the progression of HSV-1 infection relative to wild-type mice. These data are consistent with previous work showing that type II IFN and type II IFN receptors do not affect the mortality of female 129 Ev/Sv mice infected with HSV-1 (17). Therefore, a function for type II IFN in acute infection was apparent only when combined with deficiency of type I IFN receptors.

Consistent with our results, synergistic effects of type I and II IFNs in protecting mice from ocular infection with HSV-1 have been reported previously (33). However, the prior study also showed that type II IFN alone conferred resistance to HSV-1. In the previous work, eyes were treated with IFN(s) before viral infection. Therefore, the data for type II IFN-mediated resistance may be based upon either supraphysiologic levels of this cytokine or potential effects that are independent of the type II IFN receptor (12). Nevertheless, our data agree with their conclusions that complementary effects of both types of IFN (41) are needed for host immunity to acute HSV-1 infection.

The importance of type I IFNs in the immune response to herpesvirus was emphasized by a recent study of two infants with homozygous deficiency of Stat1 (11), a component of transcription complexes that mediate signaling through type I and II IFN receptors (37). One patient died of systemic infection and recurrent encephalitis from herpes simplex virus infection, while the other patient died from an undefined viral-type illness. In both cases, signaling through type I and II IFN receptors was disrupted. By comparison, patients with isolated mutations in type II IFN receptors (4) or a heterozygous Stat1 mutation that only affects type II IFN signaling (10) are susceptible to mycobacterial but not viral infections. These observations in human patients demonstrate the clinical relevance of our mouse model system and are consistent with our data for the roles of type I and II IFNs in an effective host immune response to HSV-1.

The mechanism(s) through which absence of type I IFN receptors permits systemic dissemination of HSV-1 is currently unknown. Although virus was detected in the blood and serum of IFN $\alpha/\beta/\gamma$ $R^{-/-}$ mice, the presence of luciferase activity in the lymph nodes and organs indicates that we are detecting viral replication in cells and not free viral particles. Luciferase requires ATP to produce bioluminescence from luciferin (45), so this reaction does not occur in extracellular virus (8). However, these results did not define the specific cell types that are infected at various sites. Type I IFNs could prevent infection of visceral organs by limiting the inherent permissivity to HSV-1. Alternatively, IFNs could limit trafficking of virus to sites that normally are fully permissive to HSV-1 replication, thereby eliminating systemic infection. Further studies are needed to identify cell types infected in IFN $\alpha/\beta/\gamma$ $R^{-/-}$ and IFN $\alpha/\beta/\gamma$ $R^{-/-}$ mice and distinguish between these non-mutually exclusive functions of IFNs.

In mice lacking type I IFN receptors, our data indicated that HSV-1 spread from local epithelial infection to regional lymph nodes and then to parenchymal organs, suggesting that dissemination was at least partially dependent on the lymphatic system. Spread of virus could be mediated by dendritic cells, the first antigen-presenting cells to encounter HSV-1 during epithelial or mucosal infection (31). After antigenic stimulation, dendritic cells mature and enter lymph nodes via afferent lymphatic vessels. Dendritic cells normally are permissive for infection but not replication of HSV-1 (34), and virus does not appear to replicate within draining lymph nodes (6). However, the absence of type I IFN receptors potentially could permit viral replication within dendritic cells and facilitate dissemination from lymph nodes to parenchymal organs.

Signaling through type II IFN receptors links innate immunity to the adaptive immune response to viral infection. Among the biological responses mediated by type II IFN are induction of chemokines, including CXCL9, CXCL10, and CXCL11 (24). These chemokines bind to the CXCR3 receptor that is expressed on activated T cells, NK cells, and plasmacytoid and myeloid dendritic cells, thereby regulating migration and adhesion of immune effector cells (1, 5, 22). Mice genetically deficient in CXCL10 have impaired production and recruitment of effector T cells to sites infected with mouse hepatitis virus, resulting in impaired clearance of virus (9). Although there are redundant pathways for induction of these chemokines (13), loss of type II IFN signaling could affect trafficking of cytotoxic T lymphocytes in response to HSV-1 infection. Abnormal recruitment of T cells potentially may contribute to the phenotypic differences that we observed between IFN $\alpha/\beta/\gamma$ $R^{-/-}$ and IFN α/β $R^{-/-}$ mice. To investigate this hypothesis, we plan to use bioluminescence imaging to monitor spatial and temporal localization of T cells in living mice infected with HSV-1. This general imaging strategy has been used previously to study migration of T cells to tumors or sites of bacterial infection in mouse models (reviewed in reference 25).

The phenotypes produced by HSV-1 infection in mouse models are affected by the strain of virus and mouse as well as the gender and age of the animals (17, 27, 29, 44). Our previous studies have shown that replication of the reporter virus and wild-type strain KOS are essentially identical in cultured Vero cells and outbred CD-1 mice (39, 40). Therefore, it is

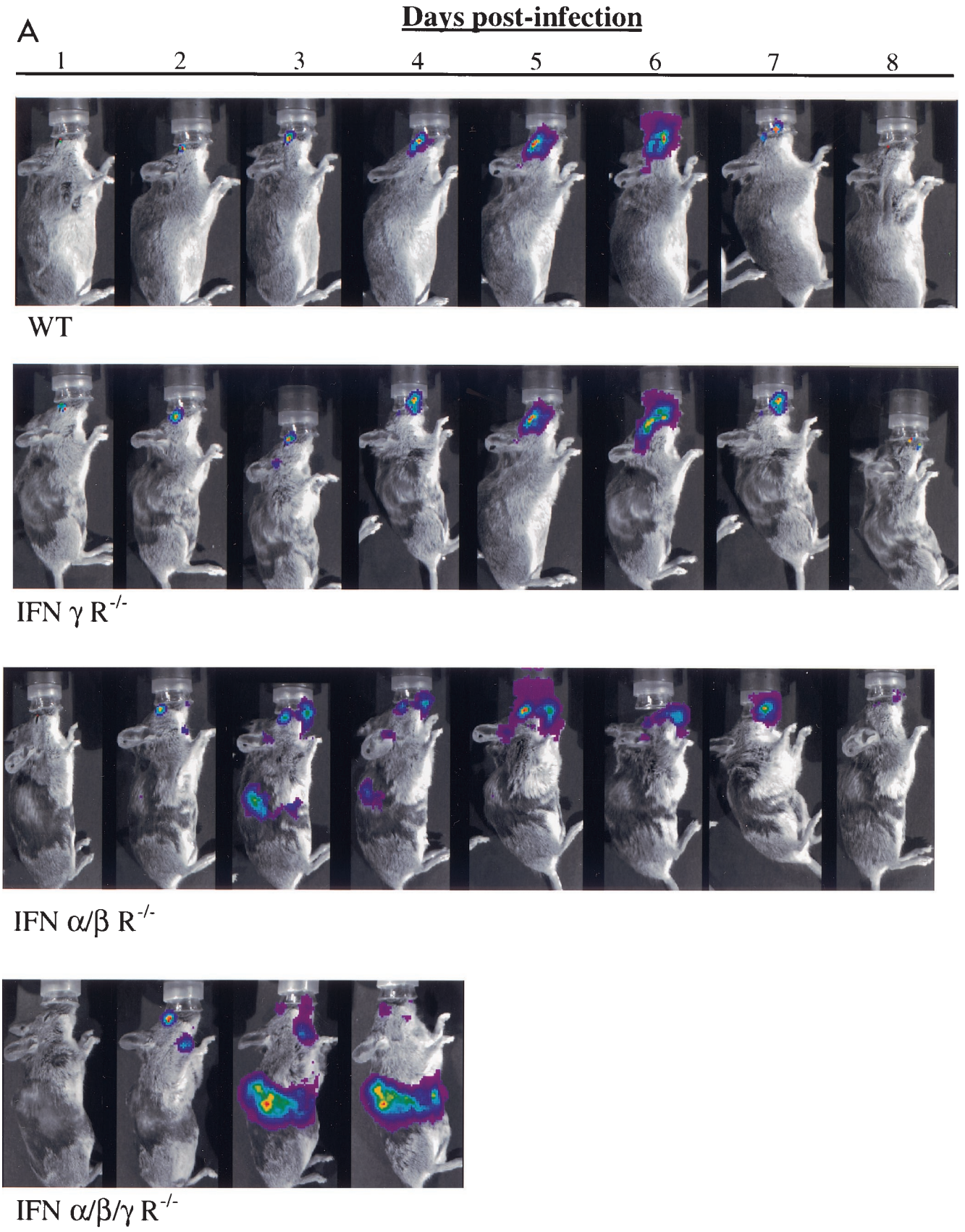
A
Days post-infection
1
2
3
4
5
6
7
8
WT
IFN γ R-/-
IFN α/β R-/-
IFN α/β/γ R-/-

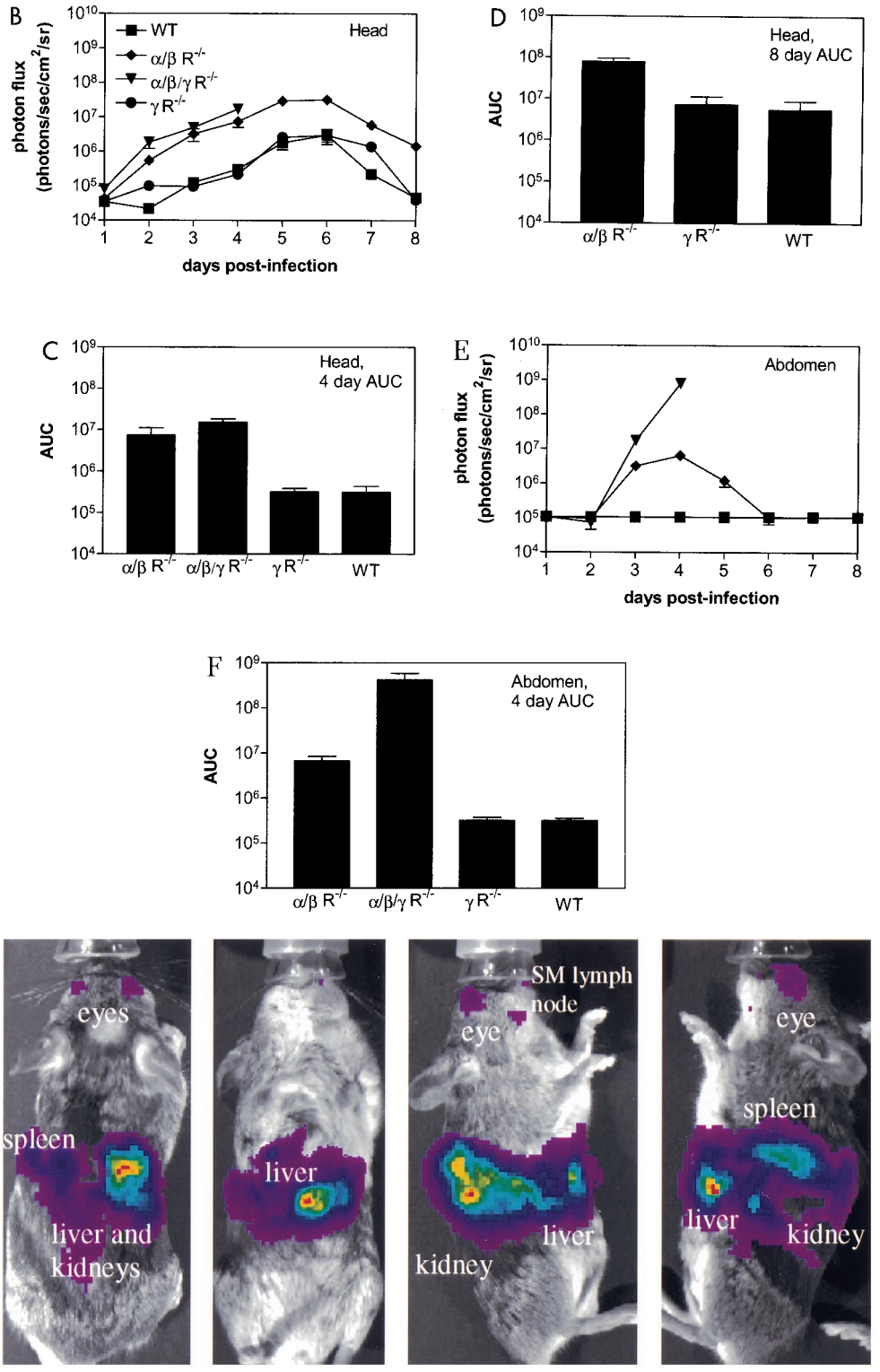

FIG. 6. Tracking viral replication and localization in wild-type (WT), IFN $\alpha/\beta/\gamma$ $R^{-/-}$, IFN α/β $R^{-/-}$, and IFN γ $R^{-/-}$ mice following ocular infection with 2×10^6 PFU KOS/dlux/oriL ($n = 5$ for each genotype). Bioluminescence imaging was performed daily for 8 days postinfection, and a representative mouse from each genotype is shown (A). Images are presented with a standardized minimum threshold for bioluminescence, but peak values for light emission varied based on relative amounts of viral replication and luciferase activity. Photon flux was quantified by region-of-interest analysis (B, E) and AUC (C, D, and F) of the head (B to D) and abdomen (E to F), respectively. The AUC for head bioluminescence was calculated over 4 and 8 days postinfection, corresponding to the duration of survival for IFN $\alpha/\beta/\gamma$ $R^{-/-}$ animals and the total length of the experiment, respectively. The AUC for abdominal photon flux was calculated only for the first 4 days postinfection. (G) Images from dorsal, ventral, and both lateral projections of an IFN $\alpha/\beta/\gamma$ $R^{-/-}$ mouse 4 days postinfection localized viral infection to multiple organs and tissues, as labeled. SM, submandibular lymph node.

unlikely that differences in viral replication and dissemination among wild-type and various IFN receptor-deficient mice are due to attenuation of strain KOS. Because strain KOS did not kill wild-type animals, our model system reproduces the typical nonlethal outcome of infection in humans. In addition, detection of genes and signaling pathways that affect susceptibility to HSV-1 is facilitated by using a nonlethal strain, compared with studying more virulent HSV-1 strains that kill a large percentage of wild-type animals. While a more virulent strain probably would produce greater lethality in all genotypes, extensive spread of virus outside the nervous system would not necessarily also occur if infection progressed more rapidly. Further investigation will be needed to establish how IFN receptors affect the dissemination and lethality of virus in mice infected with more virulent strains of HSV-1 and determine if factors such as gender and age alter the systemic spread of virus in this model.

Compared with traditional assays of virus-host pathogenesis that require sacrifice of animals and tissue harvesting at multiple time points, the current study confirmed numerous strengths of bioluminescence imaging for investigating viral disease in mouse models. By enabling repetitive imaging, spatial and temporal progression of viral infection could be monitored in the same animals over time, limiting the number of animals needed to obtain robust data sets. Relative differences in the amounts of virus were quantified noninvasively by photon flux, so differences in viral replication at a given site could be determined in the context of defined host immune deficiencies. Bioluminescence imaging also allowed the entire intact mouse to be monitored for viral replication, greatly reducing the possibility that important sites of viral replication were missed because appropriate tissues were not sampled.

However, this study also showed potential limitations of bioluminescence imaging for studies of pathogenesis. Currently, bioluminescence imaging collects two-dimensional images, so emitted light may be the summation of luciferase activity in more than one organ or tissue. This limitation was minimized by imaging animals in several different positions, although bioluminescence in lungs and probable intra-abdominal lymph nodes was still masked by large amounts of luciferase activity in the adjacent liver and spleen. In addition, bioluminescence imaging does not allow absolute quantification of luciferase activity because emitted light is attenuated depending on factors such as the depth of the signal from the animal surface and the pigmentation of skin or organs. Nevertheless, our data and a recent study with a recombinant luciferase-expressing Sindbis virus (8) establish bioluminescence imaging as an important technique for in vivo investigations of virus-host pathogenesis.

In conclusion, these data showed that deficiency of type I IFN receptors permitted HSV-1 to progress from localized infection to disseminated disease affecting multiple parenchymal organs. Furthermore, in the absence of type I IFN receptors, deletion of type II IFN receptors resulted in death of animals infected with HSV-1, although isolated deficiency of type II IFN receptors did not significantly affect replication or localization of virus relative to that in wild-type animals. Mice with a genetic deficiency of IFN receptors provide a model system for systemic HSV-1 infection, enabling further investigations o f components of the immune response that usually limit HSV-1 to localized epithelial infection with spread to innervating sensory neurons. The results also demonstrated the utility of bioluminescence imaging for monitoring the spatial and temporal progression of viral infection and detecting unanticipated sites of disease, enabling effects of host immunity on viral replication and tropism to be determined in living mice.

ACKNOWLEDGMENTS

We thank David Piwnica-Worms for encouragement, Kathryn Luker for helpful discussions, Matthew Smith for technical assistance, and Scott Tibbetts and Skip Virgin for providing mice for this study.

This study was funded by NIH grants RO1 EY09083, P50 CA94056, the McDonnell Center for Cellular and Molecular Neurobiology, and grant P30-EY02687 to the Department of Ophthalmology and Visual Sciences. Support from Research to Prevent Blindness to the Department of Ophthalmology and Visual Sciences and a Lew Wasserman Scholarship to David A. Leib are gratefully acknowledged.

REFERENCES

1. **Butcher, E., and L. Picker.** 1996. Lymphocyte homing and homeostasis. Science **272:**60–66.
2. **Cantin, E., D. Hinton, J. Chen, and H. Openshaw.** 1995. Gamma interferon expression during acute and latent nervous system infection by herpes simplex virus type 1. J. Virol. **69:**4898–4905.
3. **Cantin, E., B. Tanamachi, H. Openshaw, J. Mann, and K. Clarke.** 1999. Gamma interferon (IFN-γ) receptor null-mutant mice are more susceptible to herpes simplex virus type 1 infection than IFN-γ ligand null-mutant mice. J. Virol. **73:**5196–5200.
4. **Casanova, J., and L. Abel.** 2002. Genetic dissection of immunity to mycobacteria: the human model. Annu. Rev. Immunol. **20:**581–620.
5. **Cella, M., D. Jarrossay, F. Facchetti, O. Alebardi, H. Nakajimi, A. Lanzavecchia, and M. Colonna.** 1999. Plasmacytoid monocytes migrate to inflamed lymph nodes and produce large amounts of type I interferon. Nat. Med. **5:**919–923.
6. **Coles, R., S. Mueller, W. Heath, F. Carbone, and A. Brooks.** 2002. Progression of armed CTL from draining lymph node to spleen shortly after localized infection with herpes simplex virus 1. J. Immunol. **168:**834–838.
7. **Contag, C. H., and M. H. Bachmann.** 2002. Advances in in vivo bioluminescence imaging of gene expression. Annu. Rev. Biomed. Eng. **4:**235–260.
8. **Cook, S., and D. Griffin.** 2003. Luciferase imaging of a neurotropic viral infection in intact animals. J. Virol. **77:**5333–5338.
9. **Dufour, J., M. Dziejman, M. Liu, J. Leung, T. Lane, and A. Luster.** 2002. IFN-gamma-inducible protein 10 (IP-10; CXCL10)-deficient mice reveal a role for IP-10 in effector T cell generation and trafficking. J. Immunol. Methods **168:**3195–3204.
10. **Dupuis, S., C. Dargemont, C. Fieschi, N. Thomassin, S. Rosenzweig, J. Harris, S. Holland, R. Schreiber, and J. Casanova.** 2001. Impairment of mycobacterial but not viral immunity by a germline human STAT1 mutation. Science **293:**300–303.
11. **Dupuis, S., E. Jouanguy, S. Al-Hajjar, C. Fieschi, I. Al-Mohsen, S. Al-Jumaah, K. Yang, A. Chapgier, C. Eidenschenk, P. Eid, A. Ghonaium, H. Tufenkeji, H. Frayha, S. Al-Gazlan, H. Al-Rayes, R. Schreiber, I. Gresser, and J. Casanova.** 2003. Impaired response to interferon-alpha/beta and lethal viral disease in human STAT1 deficiency. Nat. Genet. **33:**388–391.
12. **Espejo, C., M. Penkowa, I. Saez-Torres, J. Xaus, A. Celeda, X. Montalban, and E. Martinez-Caceres.** 2001. Treatment with anti-interferon-gamma monoclonal antibodies modifies experimental autoimmune encephalomyelitis in interferon-gamma receptor knockout mice. Exp. Neurol. **172:**460–468.
13. **Farber, J.** 1997. Mig and IP-10: CXC chemokines that target lymphocytes. J. Leukoc. Biol. **61:**246–257.
14. **Farrar, M., and R. Schreiber.** 1993. The molecular cell biology of interferon-gamma and its receptor. Annu. Rev. Immunol. **11:**571–611.
15. **Fujii, S., K. Shimizu, M. Kronenberg, and R. Steinman.** 2002. Prolonged IFN-gamma-producing NKT response induced with alpha-galactosylceramide-loaded DCs. Nat. Immunol. **3:**867–874.
16. **Furio, M., and C. Wordell.** 1985. Treatment of infectious complications of acquired immunodeficiency syndrome. Clin. Pharm. **4:**539–554.
17. **Han, X., P. Lundberg, B. Tanamachi, H. Openshaw, J. Longmate, and E. Cantin.** 2001. Gender influences herpes simplex virus type 1 infection in normal and gamma interferon-mutant mice. J. Virol. **75:**3048–3052.
18. **Katze, M., Y. He, and M. J. Gale.** 2002. Viruses and interferon: a fight for supremacy. Nat. Rev. Immunol. **2:**675–687.
19. **Kimberlin, D., C. Lin, R. Jacobs, D. Powell, L. Frenkel, W. Gruber, M. Rathore, J. Bradley, P. Diaz, M. Kumar, A. Arvin, K. Gutierrez, M. Shelton,**

L. Weiner, J. Sleasman, T. de Sierra, S. Soong, J. Kiell, F. Lakeman, and R. Whitley. 2001. Natural history of neonatal herpes simplex virus infections in the acyclovir era. Pediatrics **108:**223–229.
20. **Leib, D.** 2002. Counteraction of interferon-induced antiviral responses by herpes simplex viruses. Curr. Top. Microbiol. Immunol. **269:**171–185.
21. **Leib, D., T. Harrison, K. Laslo, M. Machalak, N. Moorman, and H. Virgin.** 1999. Interferons regulate the phenotype of wild-type and mutant herpes simplex viruses in vivo. J. Exp. Med. **189:**663–672.
22. **Loetscher, M., B. Gerber, P. Loetscher, S. Jones, L. Piali, I. Clark-Lewis, M. Baggiolini, and B. Moser.** 1996. Chemokine receptor specific for IP10 and mig: structure, function, and expression in activated T-lymphocytes. J. Exp. Med. **184:**963–969.
23. **Luker, G., J. Bardill, J. Prior, C. Pica, D. Piwnica-Worms, and D. Leib.** 2002. Noninvasive bioluminescence imaging of herpes simplex virus type 1 infection and therapy in living mice. J. Virol. **76:**12149–12161.
24. **Mach, F., A. Sauty, A. Iarossi, G. Sukhova, K. Neote, P. Libby, and A. Luster.** 1999. The interferon-γ inducible CXC chemokines IP-10, Mig, and I-TAC are differentially expressed by human atheroma-associated cells: implications for lymphocyte recruitment in atherogenesis. J. Clin. Investig. **104:**1041–1050.
25. **Mandl, S., C. Schimmelpfennig, M. Edinger, R. Negrin, and C. Contag.** 2002. Understanding immune cell trafficking patterns via in vivo bioluminescence imaging. J. Cell. Biochem. Suppl. **39:**239–248.
26. **Muller, U., U. Steinhoff, L. Reis, S. Hemmi, J. Pavlovic, R. Zinkernagel, and M. Aguet.** 1994. Functional role of type I and type II interferons in antiviral defense. Science **264:**1918–1921.
27. **Norose, K., A. Yano, X. Zhang, E. Blankenborn, and E. Heber-Katz.** 2002. Mapping of genes involved in murine herpes simplex virus keratitis: identification of genes and their modifiers. J. Virol. **76:**3502–3510.
28. **Ohteki, T., T. Fukao, K. Suzue, C. Maki, M. Ito, M. Nakamura, and S. Koyasu.** 1999. Interleukin 12-dependent interferon gamma production by CD8alpha+ lymphoid dendritic cells. J. Exp. Med. **189:**1981–1986.
29. **Perng, G., K. Mott, N. Osorio, A. Yukht, S. Salina, O. Nguyen, A. Nesburn, and S. Wechsler.** 2002. Herpes simplex virus type 1 mutants containing the KOS strain ICP34.5 gene in place of the McKrae ICP34.5 gene have McKrae-like spontaneous reactivation but non-McKrae-like virulence. J. Gen. Virol. **83:**2933–2942.
30. **Pillay, D., M. Lipman, C. Lee, M. Johnson, P. Griffiths, and J. McLaughlin.** 1993. A clinico-pathological audit of opportunistic viral infections in HIV-infected patients. AIDS **7:**969–974.
31. **Pollara, G., K. Speidel, L. Samady, M. Rajpopat, Y. McGrath, J. Ledermann, R. Coffin, D. Katz, and B. Chain.** 2003. Herpes simplex virus infection of dendritic cells: balance among activation, inhibition, and immunity. J. Infect. Dis. **187:**165–178.
32. **Rader, K., C. Ackland-Berglund, J. Miller, J. Pepose, and D. Leib.** 1993. In vivo characterization of site-directed mutations in the promoter of the herpes simplex virus type 1 latency-associated transcripts. J. Gen. Virol. **74:**1859–1869.
33. **Sainz, B. J., and W. Halford.** 2002. Alpha/beta interferon and gamma interferon synergize to inhibit the replication of herpes simplex virus type 1. J. Virol. **76:**11541–11550.
34. **Samady, L., E. Costigliola, L. MacCormac, Y. McGrath, S. Cleverley, C. E. Lilley, J. Smith, D. S. Latchman, B. Chain, and R. S. Coffin.** 2003. Deletion of the virion host shutoff protein (vhs) from herpes simplex virus (HSV) relieves the viral block to dendritic cell activation: potential of vhs$^-$ HSV vectors for dendritic cell-mediated immunotherapy. J. Virol. **77:**3768–3776.
35. **Samuel, C.** 1998. Reoviruses and the interferon system. Curr. Top. Microbiol. Immunol. **233:**125–145.
36. **Smith, P., R. Wolcott, R. Chervenak, and S. Jennings.** 1994. Control of acute cutaneous herpes simplex virus infection: T cell-mediated viral clearance is dependent upon interferon-gamma (IFN-gamma). Virology **202:**76–88.
37. **Stark, G., I. Kerr, B. Williams, R. Silverman, and R. Schreiber.** 1998. How cells respond to interferons. Annu. Rev. Biochem. **67:**227–264.
38. **Su, Y., J. Oakes, and R. Lausch.** 1990. Ocular avirulence of a herpes simplex virus type I strain is associated with heightened sensitivity to alpha/beta interferon. J. Virol. **64:**2187–2192.
39. **Summers, B., and D. Leib.** 2002. Herpes simplex virus type 1 origins of DNA replication play no role in the regulation of flanking promoters. J. Virol. **76:**7020–7029.
40. **Summers, B., T. Margolis, and D. Leib.** 2001. Herpes simplex virus type 1 corneal infection results in periocular disease by zosteriform spread. J. Virol. **75:**5069–5075.
41. **Taniguchi, T., and A. Takaoka.** 2001. A weak signal for strong responses: interferon-alpha/beta revisited. Nat. Rev. Mol. Cell. Biol. **2:**378–386.
42. **Tsunobuchi, H., H. Nishimura, F. Goshima, T. Daikoku, Y. Nishiyama, and Y. Yoshikai.** 2000. Memory-type CD8+ T cells protect IL-2 receptor alpha-deficient mice from systemic infection with herpes simplex virus type 2. J. Immunol. **165:**4552–4560.
43. **Tsunobuchi, H., H. Nishimura, F. Goshima, T. Daikoku, H. Suzuki, Y. Nishiyama, and Y. Yoshikai.** 2000. A protective role of interleukin-15 in a mouse model for systemic infection with herpes simplex virus. Virology **275:**57–66.
44. **Vollstedt, S., M. Franchini, H. Hefti, B. Odermatt, M. O'Keefe, G. Alber, B. Glanzmann, M. Riesen, M. Ackermann, and M. Suter.** 2003. Flt3 ligand-treated neonatal mice have increased innate immunity against intracellular pathogens and efficiently control virus infections. J. Exp. Med. **197:**575–584.
45. **Wilson, T., and J. W. Hastings.** 1998. Bioluminescence. Annu. Rev. Cell Dev. Biol. **14:**197–230.